Sensors International 5 (2024) 100252

Contents lists available at ScienceDirect

Sensors International

journal homepage: www.keaipublishing.com/en/journals/sensors-international

Synthesis and characterization of citrate-capped gold nanoparticles and their application in selective detection of creatinine (A kidney biomarker)

Akriti Tirkey, Punuri Jayasekhar Babu *

Biomaterials and Bioengineering Research Laboratory, Department of Biotechnology, Mizoram University, Pachhunga University College Campus, Aizawl, 796001, Mizoram, India

ARTICLE INFO

Keywords:
Creatinine
Citrate-capped
Gold nanoparticles
Colorimetric
Spectrophotometric
Biomarker

ABSTRACT

A simple, sensitive, and highly selective detection method was developed for creatinine using citrate-capped gold nanoparticles (C-AuNPs). TEM analysis confirmed the synthesis of the C-AuNPs and they were mostly spherical in shape. FTIR data showed peaks at 3302 cm^{-1}, 1635 cm^{-1}, 1219 cm^{-1} and 771 cm^{-1} indicating the presence of O–H, C=C, C–O, C–C groups on the surface of the synthesized C-AuNPs. XRD analysis revealed peaks at 33.8, 44.4, 64.6, 77.5, and 81.6° confirming the crystalline nature of the C-AuNPs. The principle of this method is based on the aggregation of C-AuNPs induced by the creatinine molecules which has been successfully employed for the colorimetric detection of creatinine ranging from 0.3 to 0.8 μg/100 μl (3–8 ppm). The degree of aggregation of C-AuNPs was found to have a linear relationship with the concentration of creatinine which allows the development of a colour gradient based on the varying creatinine concentrations. UV–Vis spectrophotometric analysis further confirmed the selectivity of the method among different analytes such as ascorbic acid, nicotinic acid, polyvinyl pyrrolidone, glucose, uric acid, and bovine serum albumin. It has also been successfully applied for the detection of creatinine in urine mimic samples with good recovery rates. Therefore, this method can be successfully employed for both qualitative and quantitative analysis of creatinine.

1. Introduction

The increase in the rate of diseases has burdened the healthcare system for on-time and accurate diagnosis and prognosis which in turn has necessitated the requirement of a simple, improved, specific, sensitive, rapid, cost-effective, and eco-friendly method for the detection of metabolites associated with various diseases. In a quest to develop devices or methods to identify the clinically important metabolites (CIMs) associated with various diseases, the use of nanomaterials has gained significant popularity in recent years. One of its major blooming applications is the development of sensors based on nano-systems to detect CIMs and other biological molecules [1–5]. CIMs are molecules which are considered indicators of biological processes and pathological parameters that take place in the body due to abnormal changes. These metabolites act as biomarkers and their levels indicate the healthy and disease states of the body therefore, their accurate clinical measurement is exploited for diagnosis and determining the severity of a disease [4,6–8]. One of the most important CIMs is creatinine which is a well-known biomarker that indicates the health of the kidneys and is quantified for the diagnosis of chronic kidney disease [9–12]. The normal creatinine level in the serum and urine of healthy adult humans ranges from 0.5 to 1.5 mg/dl [13] and 11–26 mg/dl [14]. The detection and quantitative measurement of creatinine has already been achieved by several methods such as enzymatic assay [15], spectrophotometry [16], chromatography [17], high-pressure liquid chromatography [18], capillary zone electrophoresis [19], and mass spectroscopy [18,20–22]. Although these conventional methods are clinically relevant yet they exhibit certain challenges including poor sensitivity of the metabolite, instability of the metabolite during reaction, low reproducibility, lack of specificity by not being able to distinguish interferences, high detection limits, longer detection time, and involvement of complex procedures. These limitations not only affect the accuracy but also the reliability of the results [22]. Nanotechnology-based sensors can serve as a promising alternative to overcome these drawbacks owing to their excellent properties like high surface area-to-volume ratio, high absorption capacity, and increased catalytic activity [23–25]. These properties make them suitable candidates for the fabrication of highly sensitive, specific, and improved biosensors with better stability, absorbability, and accuracy along with the ease of simplified procedure and cost-effectiveness [1].

* Corresponding author.
E-mail addresses: jayasekhar.punuri@gmail.com, punuri.iitg@gmail.com (P.J. Babu).

https://doi.org/10.1016/j.sintl.2023.100252
Received 8 July 2023; Received in revised form 11 September 2023; Accepted 12 September 2023
Available online 13 September 2023

Gold nanoparticles (AuNPs) are one of the most widely studied nanoparticles (NPs) in multiple fields including healthcare [26], textiles [27], agriculture [22], and food sectors [28]. They have been extensively used for bioimaging and biosensing applications due to their unique optical properties such as localized surface plasmon resonance (LSPR) owing to their size, compatibility, and highly tuneable morphology [2,29]. Their large surface-to-volume ratio greatly increases their sensing ability. They can also be easily synthesized through different physical, chemical, and biological methods and are inert and stable against oxidation [30]. Moreover, they overcome the limitations of conventional spectroscopy by enhancing the Raman and Rayleigh signals of various biological entities and therefore, provide a better understanding of the chemical nature of biological entities [31–33]. In recent years, several studies have reported the use of complex AuNP-based systems for the sensing and quantification of creatinine which include complex processes such as sample pre-processing or extraction [10,20,34,35]. Contrary to the earlier reports, the present study aims to report a simple and selective colorimetric and spectrophotometric method for the detection of creatinine using citrate-capped AuNPs (C-AuNPs).

2. Materials and methods

2.1. Materials

The chemicals used in this study are AR grade. The chemicals including trisodium citrate, creatinine anhydrous, bovine serum albumin (BSA), uric acid, glucose, nicotinic acid, polyvinyl pyrrolidone (PVP), ascorbic acid, calcium chloride, magnesium sulphate, sodium bicarbonate, sodium chloride, sodium dihydrogen orthophosphate, disodium hydrogen phosphate, ammonium chloride, urea, and potassium chloride were purchased from Himedia. Gold chloride trihydrate ($HAuCl_4{\cdot}3H_2O$) was acquired from Sigma. Deionized water was used for the preparation of all the solutions. Freshly prepared creatinine solution was used for all the assays.

2.2. Synthesis of citrate-capped gold nanoparticles (C-AuNPs)

The C-AuNPs were synthesized using Turkevich method [36] with slight modification. Trisodium citrate was used for the reduction of gold chloride trihydrate solution ($HAuCl_4$). It also acted as the stabilizing agent for the synthesized NPs. The brief methodology includes the heating of 500 ml of 0.25 mM $HAuCl_4$ solution to 100 °C and the addition of 15 ml of trisodium citrate (1%) solution to it under constant stirring for 30 min. The faint yellow coloured solution turned to a bright ruby-red colour indicating the reduction of gold ions to NPs.

2.3. Preparation of urine mimic

A urine mimic solution was prepared by dissolving various salts such as calcium chloride (44.5 mg), magnesium sulphate (50 mg), sodium bicarbonate (17 mg), sodium chloride (317 mg), sodium dihydrogen orthophosphate (50 mg), disodium hydrogen phosphate (5.5 mg), ammonium chloride (80.5 mg), sodium citrate (148.5 mg), uric acid (17 mg), urea (1213.5 mg), potassium chloride (225 mg), and creatinine (varying concentrations) in 100 ml deionized water [10].

2.4. Characterization of citrate capped-AuNPs

2.4.1. Ultraviolet–Visible (UV–Vis) spectroscopy

The UV–Visible absorption spectrum of the synthesized C-AuNPs was measured using a UV–Visible spectrophotometer (Multiplate reader, BioTek, EPOCH2NS). The absorbance was scanned in the range between 300 and 800 nm.

2.4.2. Transmission electron microscopy (TEM)

The morphology of the C-AuNPs was investigated using transmission electron microscopy (JEOL 2100, Jeol Ltd., Tokyo, Japan). The shape, size, and selected area electron diffraction (SAED) pattern of the C-AuNPs were studied using this method.

2.4.3. Fourier transform infrared (FTIR) spectroscopy

The FTIR spectrum of the C-AuNPs was recorded to determine its surface composition using IR affinity-1S, Shimadzu. The liquid C-AuNPs solution was used directly for the analysis. The sample was placed on the sample platform and was scanned from 500 to 4000 cm^{-1}.

2.4.4. X-ray diffraction (XRD) analysis

The x-ray diffraction analysis of the synthesized C-AuNPs was conducted to determine its crystallinity. The sample for XRD analysis was prepared using drop-casting method. A thin layer of the C-AuNPs was obtained on a microscopic glass slide by repeated deposition of the NP solution on it and drying at 50 °C in a hot air oven and was analysed using an X-ray diffractometer, D8-Advance, Bruker, IASST (Guwahati, India).

2.5. Colorimetric detection of creatinine

For the colorimetric sensing of creatinine, 100 µl of different concentrations of creatinine ranging from 0.3 to 0.8 µg (3–8 ppm) was added to 1 ml of C–AuNPs solution and gently mixed. The mixture was allowed to react and observed for any visible change in colour. The UV–Visible absorbance of the solution was measured between 300 and 800 nm. The standard concentrations of creatinine were plotted against the ratio of absorbance at 630 nm and 520 nm.

2.6. Selectivity assay for the detection of creatinine

To investigate the selectivity of the C-AuNPs reaction with creatinine, different common biological compounds such as BSA, glucose, and uric acid were tested with the AuNPs under the same conditions at a concentration of 10 µg/100 µl. Few analytes known to have similar chemical structure as creatinine such as ascorbic acid, nicotinic acid, and polyvinyl pyrrolidone (PVP) were also investigated under the same parameters. The solutions were monitored for any visual colour change and their ratio of absorbance at 630 nm and 520 nm was compared with the absorbance of creatinine in the detection system.

2.7. Selectivity and detection of creatinine in urine mimic solution

To investigate the sensing ability of the C-AuNPs in biological fluids, this method was used to determine the concentration of creatinine in urine mimic solution. The artificially prepared urine mimic sample was spiked with 0.3 µg/100 µl, 0.4 µg/100 µl and 0.8 µg/100 µl of creatinine and their absorbance was compared with the absorbance of C-AuNPs in the presence of standard creatinine solutions. The different individual components of urine mimic ($CaCl_2$-44.5 µg/100 µl, $MgSO_4$-50 µg/100 µl, $NaHCO_3$-17 µg/100 µl, NaH_2PO_4-50 µg/100 µl, NaCl-317 µg/100 µl, Na_2HPO_4-5.5 µg/100 µl, NH_4Cl-80.5 µg/100 µl, KCl-225 µg/100 µl, sodium citrate-148.5 µg/100 µl, urea-1213.5 µg/100 µl, uric acid-17 µg/100 µl) were also tested with the C-AuNPs to examine their absorbance under the same conditions in order to analyse their role as interferences in the detection system.

3. Results and discussion

3.1. Synthesis and characterization of C-AuNPs

3.1.1. UV–Visible spectroscopy and TEM analysis

The synthesis of C-AuNPs by trisodium citrate reduction was observed as the colour of the solution changed from faint yellow to ruby

red. The typical ruby red colour of the C-AuNPs is attributed to its property of localized surface plasmon resonance wherein the incident light interacts with the free electrons in the NPs resulting in a collective oscillation of electrons in the conduction band. The frequency of this collective oscillation lies within the visible region of the electromagnetic spectrum resulting in a strong SPR absorption [20,30,37,38]. In case of plasmonic NPs, UV–Visible spectroscopy provides useful insights about the different properties of NPs including their size and shape based on their absorption bands [39]. The C-AuNPs showed a sharp peak at 520 nm under UV–visible spectroscopy (Fig. 1a) which further confirmed the synthesis of C-AuNPs having sizes less than 15 nm [40]. TEM images revealed that the shape of the C-AuNPs were mostly spherical (Fig. 1b). The micrograph also showed that the C-AuNPs were well dispersed and without aggregation. High-resolution TEM indicate the presence of the lattice fringes of C-AuNPs (Fig. 1c). SAED analysis demonstrated bright circular rings corresponding to (1 1 1), (2 0 0) and (2 2 0) planes as shown in Fig. 1d which confirm the crystalline nature of the C-AuNPs [41,42].

3.1.2. FTIR and XRD analysis

The synthesized C-AuNPs were subjected to FTIR analysis which revealed peaks at 3302 cm^{-1}, 1635 cm^{-1}, 1219 cm^{-1}, and 771 cm^{-1} indicating the presence of O–H, C=C, C–O, C–C groups in the sample (Fig. 2a). The O–H group can be attributed to the presence of water molecules and O–H stretching of citrate molecules in the sample while C=C, C–O and C–C confirm the presence of citrate molecules along with the AuNPs [39,42,43]. The presence of the citrate molecules on the surface of the AuNPs serves two important functions. It helps in attaining chemical stability by lowering the surface energy of the highly active NPs and it stabilizes the NPs, thus preventing their agglomeration and maintaining the NPs in a well-dispersed state which is essential for their interaction with other molecules [38]. XRD analysis revealed peaks at 33.8°, 44.4° 64.6°, 77.5°, and 81.6° corresponding to the standard Bragg reflections of 111, 200, 220, 311, and 222 suggesting the face center cubic lattice structure of the synthesized C-AuNPs, confirming their crystalline nature (Fig. 2b). [42,44,45].

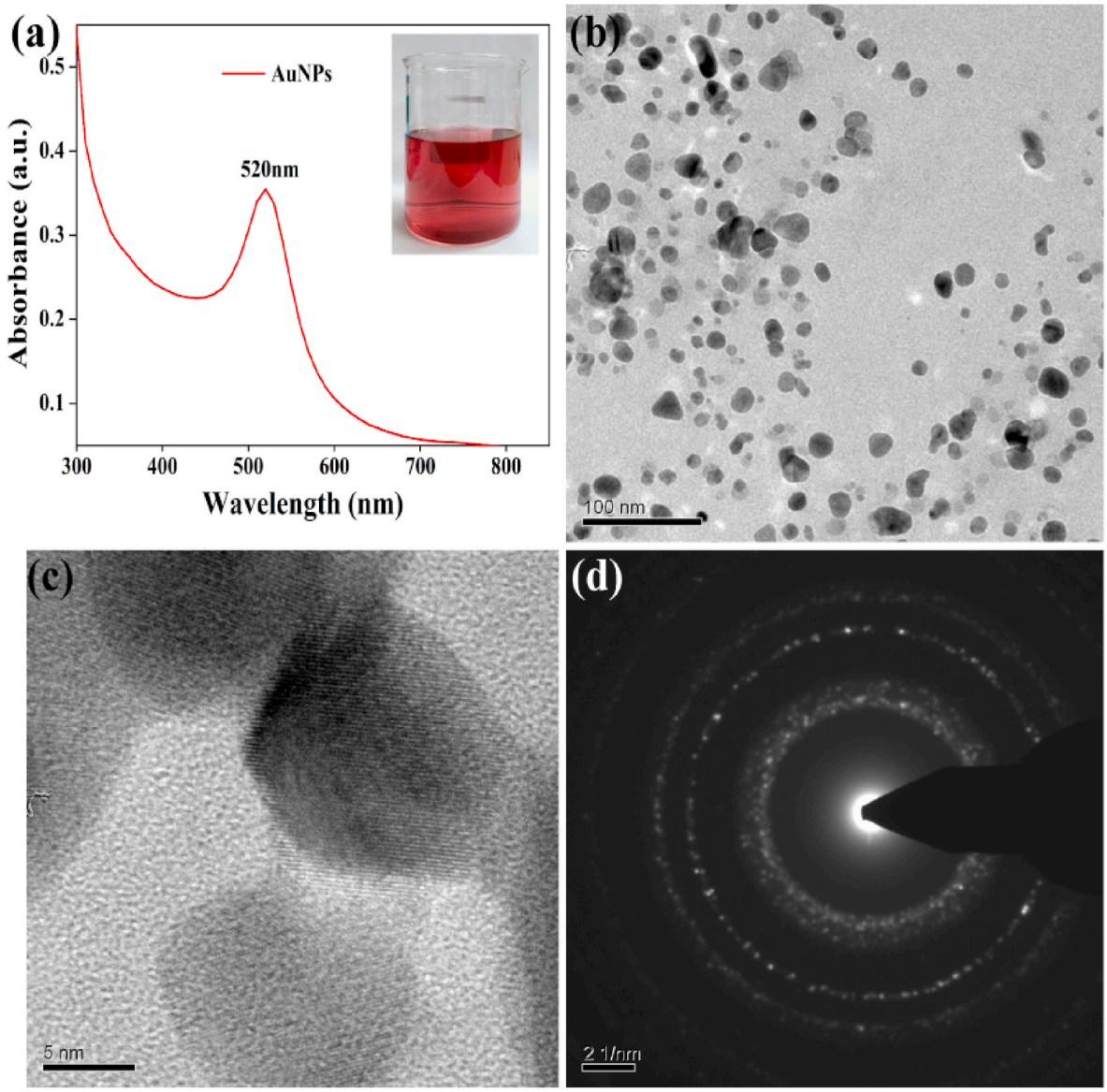

Fig. 1. **(a)** UV–Visible spectrum of the C- AuNPs showing a peak at 520 nm [Inset: Citrate capped-AuNPs solution]. **(b)** TEM image of C-AuNPs. **(c)** HR-TEM image of C-AuNPs. **(d)** SAED pattern of C-AuNPs.

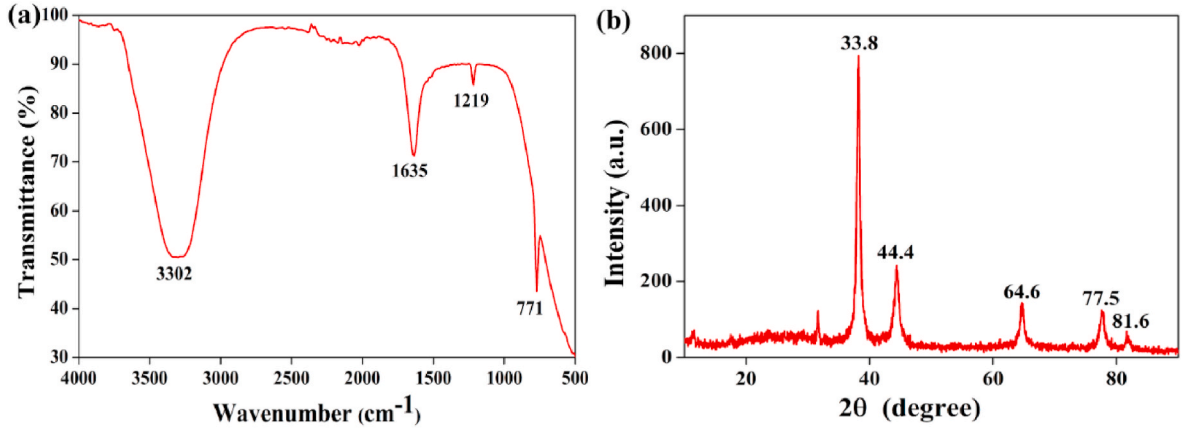

Fig. 2. **(a)** FTIR spectrum of the C-AuNPs showing peaks at 3302 cm^{-1}, 1635 cm^{-1}, 1219 cm^{-1} and 771 cm^{-1}. **(b)** XRD pattern of C-AuNPs depicting peaks at 33.8°, 44.4° 64.6°, 77.5°, and 81.6°.

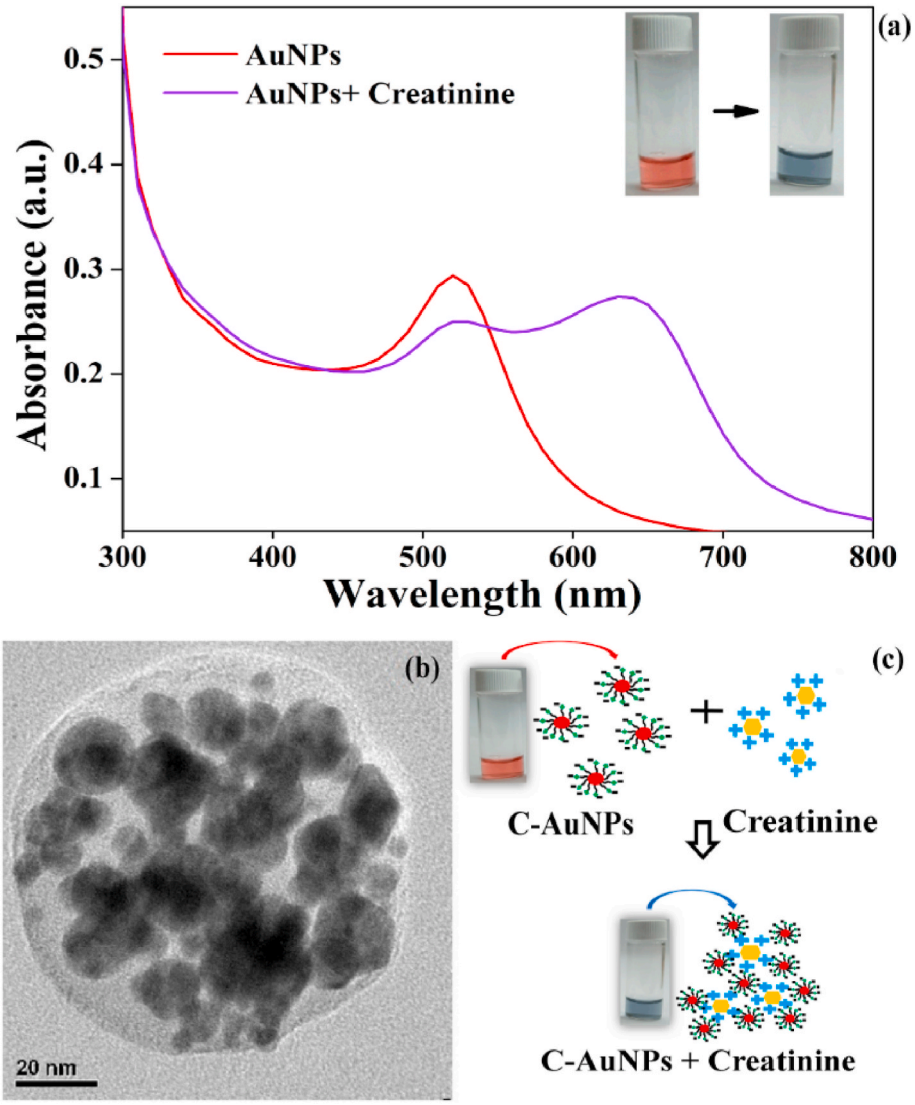

Fig. 3. **(a)** UV–visible absorption spectra of C-AuNPs and C-AuNPs + creatinine (0.8 μg/100 μl or 8 ppm). [Inset: Colour change observed in C-AuNPs from red to blue in the presence of creatinine]. **(b)** TEM image of aggregated C-AuNPs in the presence of creatinine. **(c)** Schematic diagram of reaction between C-AuNPs and creatinine.

3.2. Reaction between C-AuNPs and creatinine

Upon addition of 0.8 μg/100 μl (8 ppm) creatinine solution to 1 ml of C-AuNPs solution, a colour change was observed from red to blue (Fig. 3a Inset). This change in colour was a result of the aggregation of dispersed C-AuNPs which was induced by creatinine. This can be supported by the TEM data shown in Fig. 3b. The aggregation of C-AuNPs led to a change in the LSPR of the C-AuNPs resulting in the development of blue colour due to interparticle plasmon coupling. The change in LSPR is influenced by the size, morphology, interparticle distance, and extent of aggregation of the NPs [46,47]. The UV–Visible spectrophotometric analysis of C-AuNPs showed a sharp peak at 520 nm, while in the presence of creatinine, 2 peaks, a small peak at 520 nm and another broad peak at 630 nm were observed as shown in Fig. 3a. The peak at 630 nm was a result of the red shift in the maximum absorbance wavelength caused due to the aggregation of C-AuNPs. This is attributed to the sensitivity of the LSPR frequency to the proximity of other NPs which results in a significant bathochromic shift in the absorption maxima (from 520 nm to 630 nm) and broadening in the surface plasmon band [47]. The precise mechanism of interaction between the C-AuNPs and the creatinine molecules has not been established. However, the reaction between them may be explained based on their surface charges as shown in the Fig. 3c. The citrate capping imparts a strong negative charge to the C-AuNPs which generates natural affinity towards the positively charged creatinine molecules. Due to these charge-induced electrostatic forces of attraction, cationic creatinine molecules might bind to the anionic C-AuNPs, resulting in the overall neutralization of the charges on the C-AuNPs, and further decreasing their inter-particle distance which in turn causes the aggregation of the C-AuNPs [34]. Fig. 4 shows a schematic diagram to depict the mechanism of creatinine detection with citrate-capped gold nanoparticles.

3.3. Colorimetric detection of creatinine

In the presence of varying concentrations of creatinine ranging from 0.3 to 0.8 μg/100 μl (3–8 ppm) in C–AuNP solution, a gradient of different colour changes was observed (Fig. 5a). The colour of the C–AuNP solution darkened as the concentration of creatinine was increased, yielding a dark blue colour at 0.8 μg/100 μl (8 ppm). A saturation in the development of colour was observed beyond 0.8 μg/100 μl (8 ppm) of creatinine. Therefore, the concentration range for the detection of creatinine in this method was selected from 0.3 to 0.8 μg/100 μl (3–8 ppm). The change in the colour of the C-AuNPs in the presence of creatinine was supported by the UV–Visible absorbance spectra data (Fig. 5b) which showed a red shift in the peak from 520 nm to 630 nm due to the aggregation of C-AuNPs. Also, the graph depicts a gradual decrease in the peak intensity at 520 nm and a simultaneous increase in the peak at 630 nm with the increase in creatinine concentration. This simultaneous decrease and increase in the peak intensity of synthesized C-AuNPs at 520 nm and 630 nm respectively, is indicative of the increase in the degree of aggregation with the increasing concentrations of creatinine from 3 to 8 ppm (where 3 ppm has the lowest peak intensity and 8 ppm has the highest peak intensity at 630 nm). For the quantitative measurement of creatinine in the C–AuNP solution, a standard calibration curve was plotted using standard creatinine concentrations against the ratio of absorbance at 630 nm and 520 nm (Fig. 5c). The standard calibration curve showed a linear relationship between the creatinine concentration and the absorbance with a reliable R^2 value of 0.988 in the selected range. Therefore, this method can be successfully employed for the detection and quantification of unknown concentrations of creatinine.

3.4. Selectivity assay for the detection of creatinine

In order to assess the selectivity of this detection mechanism, different analytes having structures similar to creatinine such as ascorbic acid, nicotinic acid, polyvinyl pyrrolidone (PVP) and some common compounds present in biological fluids including glucose, uric acid and bovine serum albumin (BSA) were tested under the same conditions. No colour change was observed in the C–AuNP solution in the presence of these analytes, even at a significantly higher concentration (10 μg/100 μl or 100 ppm) than creatinine (0.8 μg/100 μl or 8 ppm). The colour of the C–AuNP solution remained unchanged and stable even after 24 h indicating the high selectivity and specificity of the C-AuNPs towards creatinine (Fig. 6a). To further confirm the selectivity of the assay, the absorption ratio at 630 nm and 520 nm of the C-AuNPs in the presence of creatinine (0.8 μg/100 μl or 8 ppm) and in the presence of the different analytes (10 μg/100 μl or 100 ppm) was investigated. Fig. 6b demonstrates that creatinine exhibited significantly higher absorption values compared to the other tested analytes, confirming the use of synthesized C–AuNPs for the selective detection of creatinine.

3.5. Selectivity and detection of creatinine in urine mimic solution

The sensitivity of the synthesized C-AuNPs in biological fluids was investigated by determining the concentration of creatinine in a urine mimic solution. The absorbance ratio at 630 nm and 520 nm of the C-AuNPs in the presence of artificially prepared urine mimic solution spiked with 0.3 μg/100 μl, 0.4 μg/100 μl and 0.8 μg/100 μl of creatinine was compared with the absorbance of C-AuNPs in the presence of the same amount of standard creatinine solutions. To further assess the selectivity of this method towards creatinine in the urine mimic solution, the different individual components of the urine mimic ($CaCl_2$-44.5 μg/100 μl, $MgSO_4$-50 μg/100 μl, $NaHCO_3$-17 μg/100 μl, NaH_2PO_4-50 μg/100 μl, NaCl-317 μg/100 μl, Na_2HPO_4-5.5 μg/100 μl, NH_4Cl-80.5 μg/100 μl, KCl-225 μg/100 μl, sodium citrate-148.5 μg/100 μl, urea-1213.5 μg/100 μl, uric acid-17 μg/100 μl) were tested with the C-AuNPs to measure their absorbance under the same conditions. The results revealed that the individual urine mimic compounds showed relatively lower absorbance in comparison with creatinine, indicating the significant selectivity and specificity of C-AuNPs towards creatinine (Fig. 7). Additionally, the creatinine concentrations determined in the urine mimic sample were comparable to the concentrations of standard creatinine solutions with recovery percentages of 93.3%, 90%, and 88.75% (Table 1). This shows that the proposed method can be successfully applied for the detection and quantification of creatinine

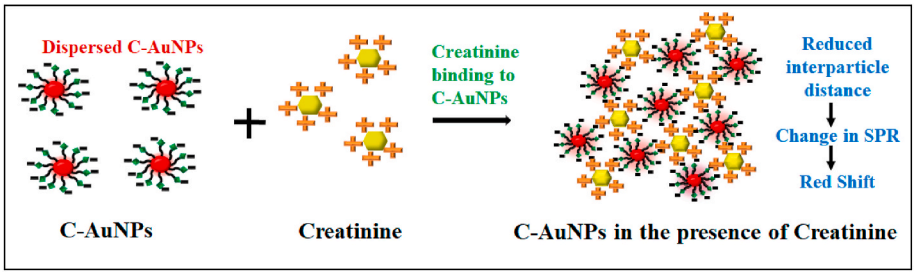

Fig. 4. Schematic diagram to depict the mechanism of creatinine detection with citrate-capped gold nanoparticles.

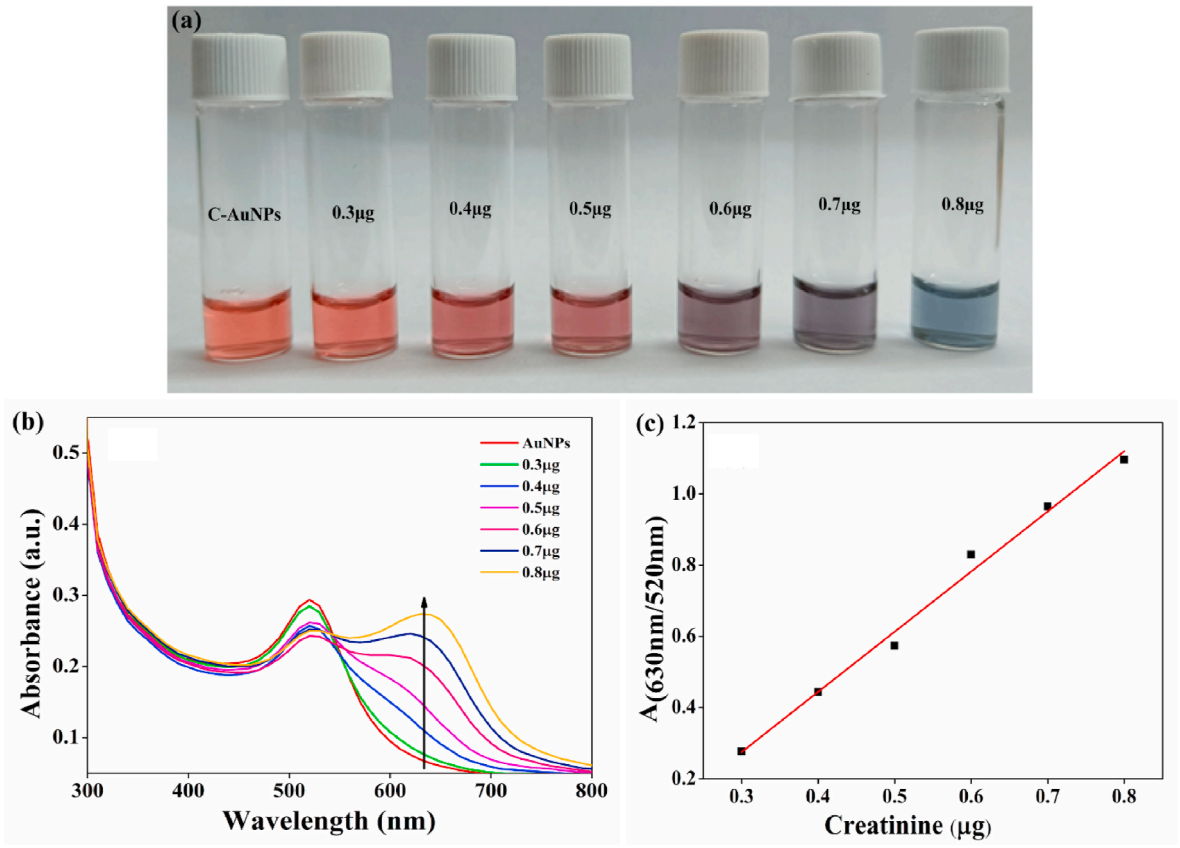

Fig. 5. **(a)** Colour change observed in C-AuNPs in the presence of different concentrations of creatinine ranging from 0.3 to 0.8 µg/100 µl (3–8 ppm). **(b)** UV–visible spectra of C-AuNPs in the presence of different concentrations of creatinine ranging from 0.3 to 0.8 µg/100 µl (3–8 ppm**). (c)** Standard calibration curve of creatinine showing a linear relationship between the concentration of creatinine and its absorbance values at 630/520 nm.

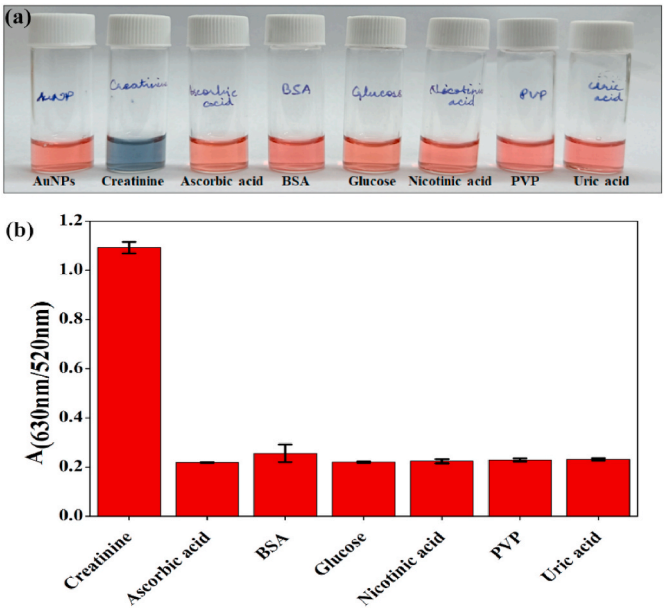

Fig. 6. **(a)** Selectivity assay of the C-AuNPs in the presence of creatinine at 0.8 µg/100 µl or 8 ppm and other analytes (ascorbic acid, BSA (bovine serum albumin), glucose, nicotinic acid, PVP (polyvinyl pyrrolidone), uric acid) at 10 µg/100 µl or 100 ppm concentration. **(b)** Absorption of the C-AuNPs at ratio of 630 nm and 520 nm in the presence of creatinine at 0.8 µg/100 µl or 8 ppm and other analytes (ascorbic acid, BSA (bovine serum albumin), glucose, nicotinic acid, PVP (polyvinyl pyrrolidone), uric acid) at 10 µg/100 µl or 100 ppm concentration.

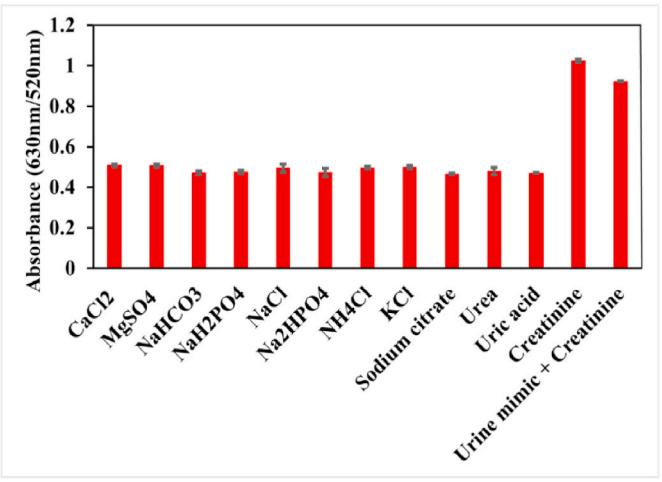

Fig. 7. Selectivity and detection of creatinine in urine mimic solution- Absorption of the C-AuNPs at ratio of 630 nm and 520 nm in the presence of individual urine mimic components ($CaCl_2$-44.5 µg/100 µl, $MgSO_4$-50 µg/100 µl, $NaHCO_3$-17 µg/100 µl, NaH_2PO_4-50 µg/100 µl, NaCl-317 µg/100 µl, Na_2HPO_4-5.5 µg/100 µl, NH_4Cl-80.5 µg/100 µl, KCl-225 µg/100 µl, sodium citrate-148.5 µg/100 µl, urea-1213.5 µg/100 µl, uric acid-17 µg/100 µl), creatinine (0.8 µg/100 µl) and urine mimic spiked with creatinine (0.8 µg/100 µl).

concentration in urine samples.

Several nanotechnology-based approaches have been explored to develop sensors for the detection and quantification of creatinine.

Table 1
Determination of creatinine using C-AuNPs in spiked urine mimic samples.

Sample	Amount of spiked (known) creatinine in urine mimic solution (in μg)	Amount of creatinine detected in urine mimic solution (in μg) ± Standard deviation	Recovery (%)
1	0.3	0.28 ± 0.002	93.3
2	0.4	0.36 ± 0.018	90
3	0.8	0.71 ± 0.005	88.75

Kalasin et al., (2020) fabricated an electrochemical sensor utilizing cuprous NPs encapsulated within polyacrylic acid gel-Cu (II). This sensor reported successful determination of creatinine concentration ranging from 200 μM to 100 mM with a lower detection limit (LOD) of 200 μM. It retained good sensitivity efficiency of 99.4% and 85% in the presence of different interferences and urine sample, respectively[48]. In another work, graphene oxide (GO), AuNPs, molybdenum disulfide NPs, and creatininase were functionalized on a singlemode fiber-multicore fiber-multimode fiber-singlemode fiber (SMF-MCF-MMF-SMF) probe to develop a LSPR-based sensor for creatinine. This sensor demonstrated a linear detection range between 0 and 2000 μM with a LOD of 128.4 μM [49]. Few studies have also reported the use of AuNPs for sensing of creatinine [34]. In a study, researchers employed label-free AuNPs for creatinine detection in urine samples, after solid-phase extraction of creatinine on a silica gel immobilized with sulfonic acid. This method displayed detection in the range of 15–40 mg/l (132.6–353.6 μM) with a LOD of 13.7 mg/l (114.9 μM) [34]. Another work by He et al., 2015 demonstrated the use of AuNPs as a colorimetric sensor for creatinine with a detection range of 0.1–20 mM and LOD of 80 μM [50]. In a similar study with citrate-capped AuNPs, colorimetry was used along with Red-Green-Blue (RGB) digital imaging. This approach revealed a LOD of 0.068 mM and a limit of quantitation (LOQ) of 0.228 mM [14]. Another work explored nano laminated gold thin film for the sensing of creatinine based on Kretschmann SPR. The developed biosensor showed a good sensitivity towards creatinine ranging from 10 to 200 mM [51]. However, the citrate-capped biosensor reported in the present study demonstrates a simple and selective method with high specificity towards creatinine even in the presence of interferents thus eliminating the requirement of additional sample processing before analysis as employed by Sittiwong and Unob. Moreover, the sensor developed in the current work shows good sensitivity towards creatinine in a range of 26.5–70.7 μM with a LOD of 26.5 μM which is significantly lower than the reported LODs in the aforementioned studies, showing its effective use in creatinine detection at very low concentrations. Table 2 summarizes a list of existing nanotechnology-based sensors for creatinine detection and a comparison of their performance with the current proposed sensor.

Moreover, the current C–AuNP based colorimetric detection method does not require sophisticated instruments, organic co-solvents, sensitive dye molecules, or enzymatic reactions, thus significantly reducing the process costs and overcoming few limitations of the existing conventional methods.

4. Conclusion

We have reported a very simple, sensitive, and highly selective approach utilizing C-AuNPs for the qualitative and quantitative detection of creatinine. Various techniques have been employed for the characterization of the synthesized C-AuNPs. The spherical shape of the NPs was determined by TEM. Furthermore, the crystallinity of the NPs and the presence of different functional groups on their surface were confirmed by XRD and FTIR analysis, respectively. The developed method allows a colorimetric detection of creatinine ranging from 0.3 to 0.8 μg/100 μl (3–8 ppm) yielding different colours based on the concentration of creatinine where the degree of aggregation of C-AuNPs is linearly proportional to the concentration of creatinine. It also allows the quantification of creatinine based on spectrophotometric analysis. Additionally, this method demonstrated excellent selectivity towards creatinine when compared with various analytes such as ascorbic acid, nicotinic acid, polyvinyl pyrrolidone, glucose, uric acid, and bovine serum albumin. This method has shown its successful application for creatinine detection in urine mimic samples with good recovery rates and specificity towards creatinine among the different urine mimic components. Therefore, this is a very reliable and specific method for the sensing and quantitative measurement of creatinine in urine mimic samples and may also be applied for the detection of creatinine in human serum.

Table 2
List of existing nanotechnology-based sensors for creatinine detection and comparison of their performance with the proposed sensor.

Nanomaterial Used	Mechanism	Detection range	LOD*	Reference
AuNPs	LSPR, Spectrophotometry	15–40 mg/l (132.6–353.6 μM)	13.7 mg/l (114.9 μM)	[34]
AuNPs	Colorimetry	0.1–20 mM	80 μM	[50]
Nano-laminated gold thin film	Kretschmann-based SPR	10–200 mM	10 mM	[51]
Cuprous NPs encapsulated with Polyacrylic gel-Cu(II)	Electrochemistry	200 μM-100 mM	200 μM	[48]
Graphene oxide-AuNPs-Molybdenum disulfide NPs-Creatininase immobilized MCF	LSPR	0–2000 μM	128.4 μM	[49]
Sodium citrate capped AuNPs	Colorimetry, RGB Digital Imaging	–	0.068 mM	[14]
Citrate capped-AuNPs	LSPR, Colorimetry, Spectrophotometry	3–8 mg/l (26.5–70.7 μM)	26.5 μM	Present work

*LOD- Limit of Detection; For Creatinine, 1 M = 113.12 g/l.

Credit authorship contribution statement

Akriti Tirkey: Investigation, Methodology, Data analysis, Data curation, Visualization, Writing – original draft. **Punuri Jayasekhar Babu:** Conceptualization, Methodology, Data analysis, Writing – review & editing, Funding acquisition and overall Supervision.

Declaration of competing interest

The authors declare that they have no known competing financial interests or personal relationships that could have appeared to influence the work reported in this paper.

Acknowledgement

The authors would also like to declare that this research is funded by the Science and Engineering Research Board (SERB), Govt. of India, vide project no: SRG/2020/002283 for providing financial support for this study.

References

[1] S. Pandit, D. Dasgupta, N. Dewan, A. Prince, Nanotechnology based biosensors and its application, Pharma Innov. 5 (2016).
[2] P.J. Babu, M. Doble, Albumin capped carbon-gold (C-Au) nanocomposite as an optical sensor for the detection of Arsenic (III), Opt. Mater. 84 (2018) 339–344.

[3] P.J. Babu, A.M. Raichur, M. Doble, Synthesis and characterization of biocompatible carbon-gold (C-Au) nanocomposites and their biomedical applications as an optical sensor for creatinine detection and cellular imaging, Sens. Actuators B-Chem. 258 (2018) 1267–1278.

[4] B.D. Malhotra, MdA. Ali, Nanomaterials in biosensors, in: Nanomaterials for Biosensors, Elsevier, 2018, pp. 1–74, https://doi.org/10.1016/B978-0-323-44923-6.00001-7.

[5] P.J. Babu, S. Saranya, Y.D. Singh, M. Venkataswamy, A.M. Raichur, M. Doble, Photoluminescence carbon nano dots for the conductivity based optical sensing of dopamine and bioimaging applications, Opt. Mater. 117 (2021), 111120.

[6] S. Akgönüllü, A. Denizli, Recent advances in optical biosensing approaches for biomarkers detection, Biosens. Bioelectron. X 100269 (2022).

[7] M. Mamas, W.B. Dunn, L. Neyses, R. Goodacre, The role of metabolites and metabolomics in clinically applicable biomarkers of disease, Arch. Toxicol. 85 (2011) 5–17, https://doi.org/10.1007/s00204-010-0609-6.

[8] B. Senf, W.-H. Yeo, J.-H. Kim, Recent advances in portable biosensors for biomarker detection in body fluids, Biosensors 10 (2020) 127, https://doi.org/10.3390/bios10090127.

[9] L.-M. Fu, C.-C. Tseng, W.-J. Ju, R.-J. Yang, Rapid paper-based system for human serum creatinine detection, Inventions 3 (2018) 34.

[10] S. Feng, R. Shi, P. Xu, J.R. Bhamore, J. Bal, S.H. Baek, C.Y. Park, J.P. Park, T. J. Park, Colorimetric detection of creatinine using its specific binding peptides and gold nanoparticles, New J. Chem. 44 (2020) 15828–15835.

[11] S.N. Prabhu, S.C. Mukhopadhyay, G. Liu, Sensors and techniques for creatinine detection: a review, IEEE Sensor. J. 22 (2022) 11427–11438, https://doi.org/10.1109/JSEN.2022.3174818.

[12] F. Wei, S. Cheng, Y. Korin, E.F. Reed, D. Gjertson, C. Ho, H.A. Gritsch, J. Veale, Serum creatinine detection by a conducting-polymer-based electrochemical sensor to identify allograft dysfunction, Anal. Chem. 84 (2012) 7933–7937, https://doi.org/10.1021/ac3016888.

[13] A.O. Hosten, BUN and Creatinine, Clin. Methods Hist. Phys. Lab. Exam, 1990.

[14] H. Findari, Mudasir, S.J. Santosa, Synthesis of sodium citrate-capped gold nanoparticles and its application for creatinine detection in urine sample by colorimetric analysis based on the red-green-blue (RGB) digital image, Nano Hybrids Compos 37 (2022) 23–31, https://doi.org/10.4028/p-5k654i.

[15] H.D. Duong, J.I. Rhee, Development of ratiometric fluorescent biosensors for the determination of creatine and creatinine in urine, Sensors 17 (2017) 2570.

[16] A. Krishnegowda, N. Padmarajaiah, S. Anantharaman, K. Honnur, Spectrophotometric assay of creatinine in human serum sample, Arab. J. Chem. 10 (2017) S2018–S2024, https://doi.org/10.1016/j.arabjc.2013.07.030.

[17] V.K. Langsi, B.A. Ashu-Arrah, N. Ward, J.D. Glennon, Synthesis and characterisation of non-bonded 1.7 μm thin-shell (TS1.7-100 nm) silica particles for the rapid separation and analysis of uric acid and creatinine in human urine by hydrophilic interaction chromatography, J. Chromatogr. A 1506 (2017) 37–44, https://doi.org/10.1016/j.chroma.2017.05.004.

[18] M. Suzuki, M. Furuhashi, S. Sesoko, K. Kosuge, T. Maeda, K. Todoroki, K. Inoue, J. Z. Min, T. Toyo'oka, Determination of creatinine-related molecules in saliva by reversed-phase liquid chromatography with tandem mass spectrometry and the evaluation of hemodialysis in chronic kidney disease patients, Anal. Chim. Acta 911 (2016) 92–99, https://doi.org/10.1016/j.aca.2016.01.032.

[19] L. Vitali, S. Gonçalves, V. Rodrigues, V.T. Fávere, G.A. Micke, Development of a fast method for simultaneous determination of hippuric acid, mandelic acid, and creatinine in urine by capillary zone electrophoresis using polymer multilayer-coated capillary, Anal. Bioanal. Chem. 409 (2017) 1943–1950, https://doi.org/10.1007/s00216-016-0142-4.

[20] H. Du, R. Chen, J. Du, J. Fan, X. Peng, Gold nanoparticle-based colorimetric recognition of creatinine with good selectivity and sensitivity, Ind. Eng. Chem. Res. 55 (2016) 12334–12340.

[21] S. Kumar, R. Singh, Recent optical sensing technologies for the detection of various biomolecules: review, Opt Laser. Technol. 134 (2021), 106620, https://doi.org/10.1016/j.optlastec.2020.106620.

[22] P.J. Babu, S. Saranya, B. Longchar, A. Rajasekhar, Nanobiotechnology-mediated sustainable agriculture and post-harvest management, Curr. Res. Biotechnol. 4 (2022) 326–336, https://doi.org/10.1016/j.crbiot.2022.07.004.

[23] P.J. Babu, A. Tirkey, T.J.M. Rao, N.B. Chanu, K. Lalchhandama, Y.D. Singh, Conventional and nanotechnology based sensors for creatinine (A kidney biomarker) detection: a consolidated review, Anal. Biochem. 114622 (2022).

[24] B. Shrestha, Nanotechnology for biosensor applications, in: Sustainable Nanotechnology for Environmental Remediation, Elsevier, 2022, pp. 513–531, https://doi.org/10.1016/B978-0-12-824547-7.00013-8.

[25] E. Heydari-Badrooei, A.A. Ensafi, Nanomaterials-based biosensing strategies for biomarkers diagnosis, a review, Biosens. Bioelectron. X 100245 (2022).

[26] X. Zhang, Gold nanoparticles: recent advances in the biomedical applications, Cell Biochem. Biophys. 72 (2015) 771–775, https://doi.org/10.1007/s12013-015-0529-4.

[27] J. Barman, A. Tirkey, S. Batra, A.A. Paul, K. Panda, R. Deka, P.J. Babu, The role of nanotechnology based wearable electronic textiles in biomedical and healthcare applications, Mater. Today Commun. 32 (2022), 104055, https://doi.org/10.1016/j.mtcomm.2022.104055.

[28] P.J. Babu, J.M.R. Tingirikari, A review on polymeric nanomaterials intervention in food industry, Polym. Bull. 80 (2023) 137–164, https://doi.org/10.1007/s00289-022-04104-6.

[29] R. Kubo, Electronic properties of metallic fine particles, I. J. Phys. Soc. Jpn. 17 (1962) 975–986, https://doi.org/10.1143/JPSJ.17.975.

[30] E. Priyadarshini, N. Pradhan, Gold nanoparticles as efficient sensors in colorimetric detection of toxic metal ions: a review, Sensor. Actuator. B Chem. 238 (2017) 888–902, https://doi.org/10.1016/j.snb.2016.06.081.

[31] J.T. Krug, G.D. Wang, S.R. Emory, S. Nie, Efficient Raman enhancement and intermittent light emission observed in single gold nanocrystals, J. Am. Chem. Soc. 121 (1999) 9208–9214, https://doi.org/10.1021/ja992058n.

[32] S. Nie, S.R. Emory, Probing single molecules and single nanoparticles by surface-enhanced Raman scattering, Science 275 (1997) 1102–1106, https://doi.org/10.1126/science.275.5303.1102.

[33] L. Rodríguez-Lorenzo, R.A. Álvarez-Puebla, F.J.G. de Abajo, L.M. Liz-Marzán, Surface enhanced Raman scattering using star-shaped gold colloidal nanoparticles, J. Phys. Chem. C 114 (2010) 7336–7340, https://doi.org/10.1021/jp909253w.

[34] J. Sittiwong, F. Unob, Detection of urinary creatinine using gold nanoparticles after solid phase extraction, Spectrochim. Acta. A. Mol. Biomol. Spectrosc. 138 (2015) 381–386, https://doi.org/10.1016/j.saa.2014.11.080.

[35] Zhu Xia, Li Bian, Liu Liu, Highly sensitive and selective colorimetric detection of creatinine based on synergistic effect of PEG/Hg2+–AuNPs, Nanomaterials 9 (2019) 1424, https://doi.org/10.3390/nano9101424.

[36] J. Turkevich, P.C. Stevenson, J. Hillier, A study of the nucleation and growth processes in the synthesis of colloidal gold, Discuss. Faraday Soc. 11 (1951) 55, https://doi.org/10.1039/df9511100055.

[37] P. Sharma, P.J. Babu, U. Bora, Sapindus mukorossi aqueous fruit extract as reducing, capping and dispersing agents in synthesis of gold nanoparticles, Micro & Nano Lett. 7 (2012) 1296–1299.

[38] G. Zhang, Functional gold nanoparticles for sensing applications, Nanotechnol. Rev. 2 (2013) 269–288, https://doi.org/10.1515/ntrev-2012-0088.

[39] S. Gurunathan, J. Han, J.H. Park, J.-H. Kim, A green chemistry approach for synthesizing biocompatible gold nanoparticles, Nanoscale Res. Lett. 9 (2014) 1–11.

[40] V. Borse, A.N. Konwar, Synthesis and characterization of gold nanoparticles as a sensing tool for the lateral flow immunoassay development, Sens. Int. 1 (2020), 100051.

[41] P.J. Babu, P. Sharma, M.C. Kalita, U. Bora, Green synthesis of biocompatible gold nanoparticles using Fagopyrum esculentum leaf extract, Front. Mater. Sci. 5 (2011) 379–387, https://doi.org/10.1007/s11706-011-0153-1.

[42] P.J. Babu, P. Sharma, S. Saranya, U. Bora, Synthesis of gold nanoparticles using ethonolic leaf extract of Bacopa monnieri and UV irradiation, Mater. Lett. 93 (2013) 431–434.

[43] J. Dong, P.L. Carpinone, G. Pyrgiotakis, P. Demokritou, B.M. Moudgil, Synthesis of precision gold nanoparticles using Turkevich method, KONA Powder Part. J. 37 (2020) 224–232.

[44] M.F. Fazaludeen, C. Manickam, I.M. Ashankyty, M.Q. Ahmed, Q.Z. Beg, Synthesis and characterizations of gold nanoparticles by Justicia gendarussa Burm F leaf extract, J. Microbiol. Biotechnol. Res. 2 (2012) 23–34.

[45] S. Krishnamurthy, A. Esterle, N.C. Sharma, S.V. Sahi, Yucca-derived synthesis of gold nanomaterial and their catalytic potential, Nanoscale Res. Lett. 9 (2014) 1–9.

[46] K.M.A. El-Nour, E.T.A. Salam, H.M. Soliman, A.S. Orabi, Gold nanoparticles as a direct and rapid sensor for sensitive analytical detection of biogenic amines, Nanoscale Res. Lett. 12 (2017) 231, https://doi.org/10.1186/s11671-017-2014-z.

[47] K. Saha, S.S. Agasti, C. Kim, X. Li, V.M. Rotello, Gold nanoparticles in chemical and biological sensing, Chem. Rev. 112 (2012) 2739–2779, https://doi.org/10.1021/cr2001178.

[48] S. Kalasin, P. Sangnuang, P. Khownarumit, I.M. Tang, W. Surareungchai, Evidence of Cu(I) coupling with creatinine using cuprous nanoparticles encapsulated with polyacrylic acid gel-Cu(II) in facilitating the determination of advanced kidney dysfunctions, ACS Biomater. Sci. Eng. 6 (2020) 1247–1258, https://doi.org/10.1021/acsbiomaterials.9b01664.

[49] M. Li, R. Singh, C. Marques, B. Zhang, S. Kumar, 2D material assisted SMF-MCF-MMF-SMF based LSPR sensor for creatinine detection, Opt Express 29 (2021), 38150, https://doi.org/10.1364/OE.445555.

[50] Y. He, X. Zhang, H. Yu, Gold nanoparticles-based colorimetric and visual creatinine assay, Microchim. Acta 182 (2015) 2037–2043, https://doi.org/10.1007/s00604-015-1546-0.

[51] P.S. Menon, F.A. Said, G.S. Mei, D.D. Berhanuddin, A.A. Umar, S. Shaari, B. Y. Majlis, Urea and creatinine detection on nano-laminated gold thin film using Kretschmann-based surface plasmon resonance biosensor, PLoS One 13 (2018), e0201228, https://doi.org/10.1371/journal.pone.0201228.